

Nitrobenzene Adsorption in Activated Carbon as Observed by NMR

L. Pel, R. M. E. Valckenborg, and K. Kopinga

Dept. of Applied Physics, Eindhoven University of Technology, 5600 MB Eindhoven, The Netherlands

F. B. Aarden and P. J. A. M. Kerkhof

Dept. of Chemical Engineering, Eindhoven University of Technology, 5600 MB Eindhoven, The Netherlands

The adsorption of nitrobenzene in activated carbon was investigated by nuclear magnetic resonance (NMR). Because of the short relaxation times and carbon is an electrically conducting material, a specially adapted NMR setup was used. It was found that during the adsorption process the nitrobenzene profiles can be scaled using the Boltzmann transformation and the overall effective diffusivity can be approximated by an exponential function of the nitrobenzene content.

Introduction

Adsorption processes form an important value-adding step in the chemical process industry. Adsorption is important in, for example, the removal of undesired components from wastewater and air streams. There are many materials, both from Nature and from synthesis, that have sorption capacity. Among the most important commercial adsorbents are activated carbon, molecular-sieve zeolites, silica gel, and activated alumina, of which the applications depend on their particular sorptive properties (Crittenden and Thomas, 1998). The activated carbons are an important group of adsorbents, which are used to recover nitrogen from air, ethene from methane and hydrogen, remove odors from gases, and in gas masks and water purification, including removal of phenol, halogenated compounds, pesticides, caprolactam, and chlorine. Often uptake experiments are used in order to study the kinetics of adsorption. In these experiments the integrated adsorption profiles are followed as a function of time, for example, by measuring the total mass of adsorbate plus adsorbent, or by measuring concentration changes in the continuous phase surrounding the adsorbent. However, a model is needed to calculate the adsorption profiles in the adsorbent itself. Such models are usually based on Fickian or Maxwell–Stefan diffusion and assume a constant effective diffusion coefficient (see, for example, Wankat, 1990). A direct measurement of the evolution of adsorption profiles with time would give considerably more information about the adsorption kinetics without *a priori* model assumptions. Schem-

mert et al. (1999a,b) used optical techniques to determine the diffusion process in zeolite. Koptug et al. (2000a,b) and Prado et al. (1999) showed that nuclear magnetic resonance (NMR) is an excellent method to study the kinetics of adsorption nondestructively and quantitatively. However, activated carbon is an electrically conducting material that creates specific problems for the NMR measurements, in particular when quantitative measurements of, for example, concentrations are performed. Standard NMR equipment cannot be used and, therefore, a specially adapted NMR setup has been built. Using this setup the adsorption of nitrobenzene in activated carbon has been studied. Based on the measured nitrobenzene profiles, the macroscopic diffusivity of nitrobenzene has been determined. Special attention is given to the various inaccuracies in the determination of the diffusivity.

Nuclear Magnetic Resonance

NMR is a magnetic-resonance technique, where the resonance condition for the nuclei is given by

$$f = \gamma B_o \quad (1)$$

In this equation f is the resonance frequency, γ is the so-called gyromagnetic ratio, and B_o is the externally applied static magnetic field. Because each type of nucleus has a specific value of γ , the method can be made sensitive to only hydrogen, and, therefore, to nitrobenzene, in this study. When a known magnetic-field gradient is applied, the resonance

Correspondence concerning this article should be addressed to L. Pel.

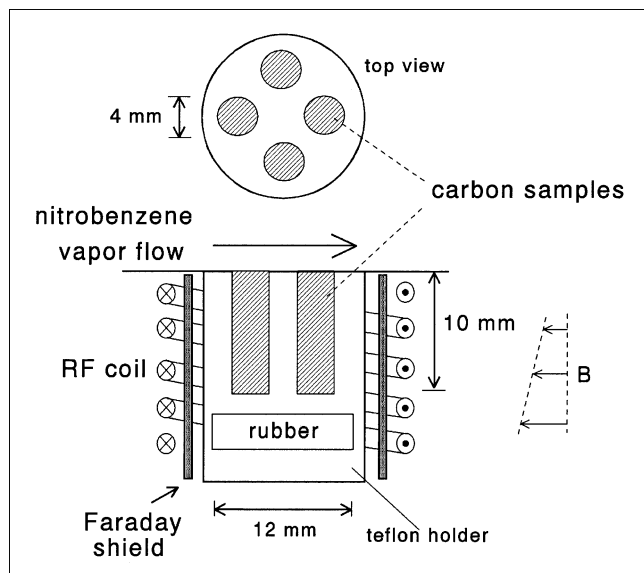


Figure 1. Experimental setup for measuring the nitrobenzene profiles during adsorption with NMR.

condition will depend on the spatial position of the nuclei and their distribution can be measured without moving the sample. The NMR measurements reported in this article were performed using the so-called spin-echo technique. Assuming a single exponential decay, the magnitude of an NMR spin-echo signal is given by (Abragam, 1962)

$$S \sim \rho[1 - \exp(-TR/T_1)]\exp(-TE/T_2) \quad (2)$$

where ρ is the proton density, T_1 is the spin-lattice (longitudinal) relaxation time, TR is the repetition time of the spin-echo experiment, T_2 is the spin-spin (transverse) relaxation time, and TE is the spin-echo time. This equation is valid if $T_1 \gg T_2$. As can be seen from Eq. 2, small T_2 values lead to a decrease of the spin-echo signal, whereas, on the other hand, small T_1 values are preferred, as this parameter limits the repetition time (usually $TR \approx 4T_1$).

The experiments described in this study were performed using an NMR apparatus especially designed for quantitative measurements in inorganic porous materials (Pel, 1995; Kopinga and Pel, 1994). The NMR probe head is shown in Figure 1. Four small cylinders of extruded activated carbon Chernviron AP4-60 with a length of 10 mm and a diameter of 4 mm are placed in a PTFE holder, the upper side of which is open (PTFE, that is, proton-free teflon does not contain any hydrogen). A saturated flow of nitrobenzene is blown over the samples, thus, creating a one-dimensional (1-D) adsorption experiment. The temperature of the sample holder during the adsorption process is 33°C, as measured independently by a thermoresistor (Pt100).

A coil, which forms part of a tuned LC circuit, is placed around the sample for creating and receiving the radio frequency fields during NMR experiments. In order to perform quantitative measurements, a Faraday shield is placed between the coil and the sample to suppress the effects of the

changes of the dielectric permittivity by variations of the nitrobenzene content. Apart from this, since carbon is electrically conducting, which leads to a significant detuning of the LC circuit, the quality factor Q of the LC circuit was made extra low, that is, on the order of 10. This low Q will decrease the signal-to-noise ratio, which has to be compensated for by increasing the number of averages of the spin-echo measurements.

The probe head is placed between the poles of an iron-cored electromagnet, which creates a static field of 0.75 T, corresponding to a resonance frequency for ^1H of 32 MHz. This low frequency was chosen to reduce possible skin effects of the electrically conducting carbon. A magnetic field gradient of 0.38 T/m is generated in the vertical direction with a pair of Anderson coils. Since we intend to determine the total nitrobenzene content, the Hahn spin-echo sequences ($90_x - \tau - 180_{\pm x}$) were kept as short as possible, that is, with $t_{90^\circ} = 12 \mu\text{s}$ and a spin-echo time of 205 μs . The 1-D resolution in this case is 1.0 mm. In order to correct for variations of the sensitivity of the NMR setup, a reference sample of silicone rubber was placed just below the carbon samples. Therefore, hydrogen concentration profiles were measured over 25 mm, which took typically 52 min using 256 averages at each position. During the measurement of a concentration profile, a time stamp was added to each point.

The absolute accuracy of the equipment was tested by measurements on various series of samples, each with a different nitrobenzene content. For this purpose the carbon samples were outgassed first for 24 h under a vacuum at 160°C. In Figure 2 the observed signal is plotted against the corresponding gravimetrically determined nitrobenzene content. As can be seen from this figure, the NMR signal varies linearly with the nitrobenzene content. A small background level is observed, which is attributed to hydrogen atoms still

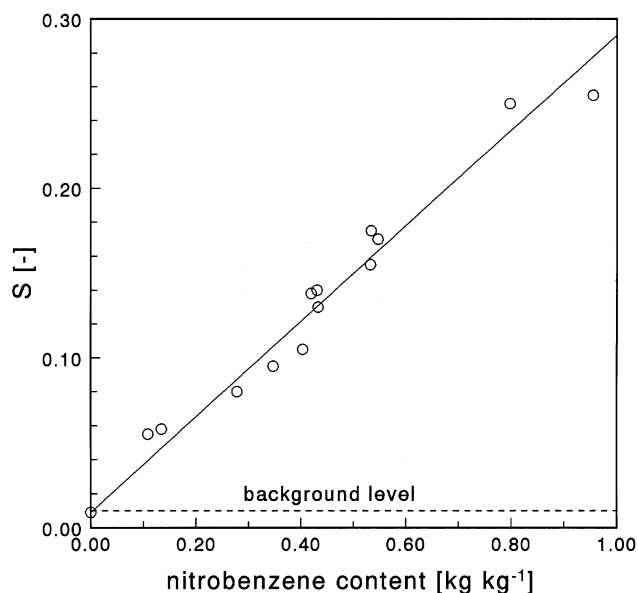


Figure 2. Measured NMR signal against the corresponding gravimetrically determined nitrobenzene content.

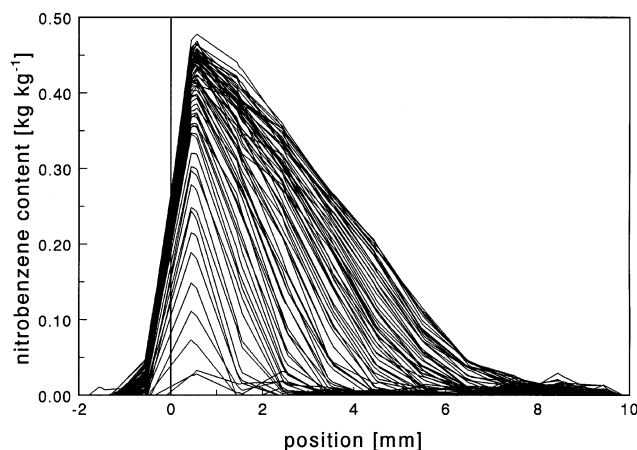


Figure 3. Measured nitrobenzene profiles during adsorption.

The time between subsequent profiles is 52 min, and the profiles are given for 70 h, that is, a total of 80 profiles.

present in the carbon after outgassing, since it is not detected when the carbon samples are removed.

Experimental Results

The nitrobenzene profiles for adsorption measured by NMR are plotted in Figure 3 for a total time of 70 h. As can be seen, initially the nitrobenzene content near the surface seems to be increasing, whereas, for this type of experiment, one would expect a constant value at the surface. Since the region in which this anomalous behavior occurs is of the same order as the 1-D resolution, this increase is probably due to an experimental artifact. We will validate this assumption later in the error analysis.

The mass transport for the 1-D isothermal problem reflecting the experiment can be described by (Bear and Bachmat, 1990; Whitaker, 1977)

$$\frac{\partial \theta}{\partial t} = \frac{\partial}{\partial x} \left(D_{\text{eff}} \frac{\partial \theta}{\partial x} \right) \quad (3)$$

In this equation θ is the actual nitrobenzene content, D_{eff} is the effective overall nitrobenzene diffusivity, which is a function of the actual nitrobenzene content, and x corresponds to the vertical direction in our experiments.

The nitrobenzene transport during adsorption can be described by Eq. 3 with the initial condition

$$\theta = \theta_0 \quad \text{for } x > 0, \quad t = 0 \quad (4)$$

where θ_0 is the initial uniform nitrobenzene content of the sample.

The boundary condition at the surface is given by

$$D_{\text{eff}} \frac{\partial \theta}{\partial x} = \beta [P_{\text{mat}}(\theta) - P_{\text{vapor}}] \quad \text{at } x = 0, \quad t > 0 \quad (5)$$

where β is the mass-transfer coefficient, P_{vapor} the vapor pressure of the nitrobenzene blown over the sample, and $P_{\text{mat}}(\theta)$ the vapor pressure in the material at the interface. The latter can be deduced from the sorption isotherm. In the case where diffusion into the material is limited by the mass transfer, as will be assumed in this experiment, this condition can be simplified to

$$P_{\text{vapor}} = P_{\text{mat}}$$

that is,

$$\theta = \theta_{\text{bound}} \quad \text{for } x = 0, \quad t > 0, \quad (6)$$

where θ_{bound} is the nitrobenzene content of the material at the surface for which $P_{\text{vapor}} = P_{\text{mat}}$.

If, for the system described by Eq. 3 and Eq. 6, the well-known Boltzmann transformation

$$\lambda = \frac{x}{\sqrt{t}} \quad (7)$$

is applied, the nonlinear diffusion equation (Eq. 3) describing the nitrobenzene transport reduces to the ordinary differential equation

$$2 \frac{d}{d\lambda} \left(D_{\text{eff}} \frac{d\theta}{d\lambda} \right) + \lambda \frac{d\theta}{d\lambda} = 0 \quad (8)$$

with boundary conditions

$$\begin{aligned} \theta &= \theta_{\text{bound}} & \text{at } \lambda &= 0 \\ \theta &= \theta_0 & \text{for } \lambda &\rightarrow \infty \end{aligned} \quad (9)$$

Equation 8, with the boundary conditions in Eq. 9, has only one solution, so the adsorption profiles at different times are related by a simple \sqrt{t} scaling. The transformed profiles are plotted in Figure 4. Here the data for $x < 1$ mm and the profiles collected during the first 16 h were not used (see also

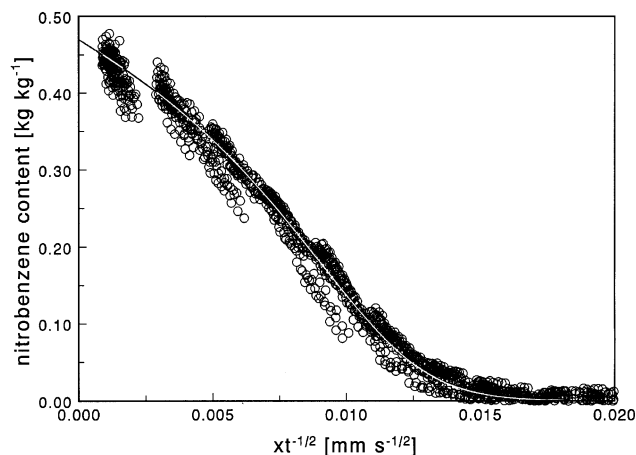


Figure 4. Boltzmann transformation of the measured nitrobenzene profiles.

The solid curve is the Boltzmann transformation of profiles that were simulated using an exponential dependence of the diffusivity on the nitrobenzene content.

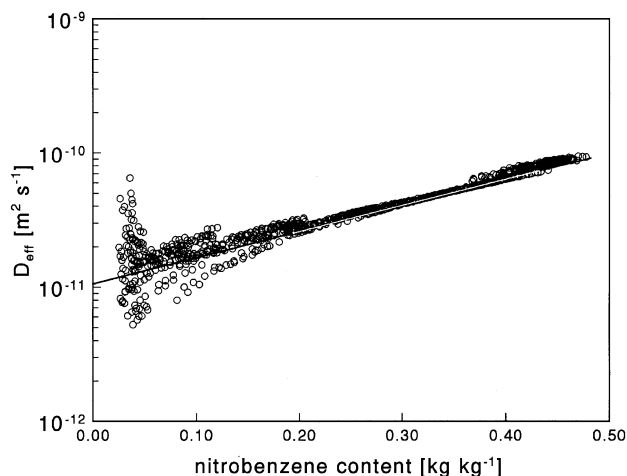


Figure 5. Effective diffusivity for adsorption as determined from the Boltzmann transformed profiles.

The solid line denotes an exponential approximation: $D_{\text{eff}} = 1.05 \times 10^{-11} \exp(4.5 \theta)$.

error analysis). As can be seen, the Boltzmann transformation yields a distinct curve, on which the data of the various profiles collapse. This indicates that the effective diffusivity does not depend on the position and supports the modeling of the nitrobenzene transport during the adsorption by a diffusion equation. It also indicates that in this case the mass-transfer coefficient is large enough, so that indeed Eq. 6 is valid.

In principle, the effective diffusivity for adsorption can be determined without *a priori* assumptions about its dependence on θ by integrating Eq. 8 with respect to λ using the boundary conditions in Eq. 9, yielding

$$D_{\text{eff}} = -\frac{1}{2} \frac{1}{\left(\frac{d\theta}{d\lambda}\right)_{\theta}} \int_{\theta_0}^{\theta} \lambda d\theta' \quad (10)$$

Using this equation, D_{eff} can be calculated numerically from the transformed experimental nitrobenzene profiles; $\lambda = f(\theta)$. Starting at the horizontal λ -axis, the data are integrated numerically down to the nitrobenzene content of interest. The resulting integral is divided by the local derivative of the averaged set of data with respect to λ at that nitrobenzene content. If this procedure is repeated over the full nitrobenzene range, the effective diffusivity D_{eff} is found as a function of nitrobenzene content. The effective diffusivity for adsorption for activated carbon obtained by this method is given in Figure 5.

As can be seen from Figure 5, the overall behavior of D_{eff} can be approximated by an exponential function, that is

$$D_{\text{eff}} = D_0 \exp(\alpha \theta) \quad (11)$$

where $D_0 = 1.05 \text{ m}^2 \text{ s}^{-1}$ and $\alpha = 4.5$.

This diffusivity is reflected by the solid line in Figure 5. Although the experimental diffusivity has considerable noise

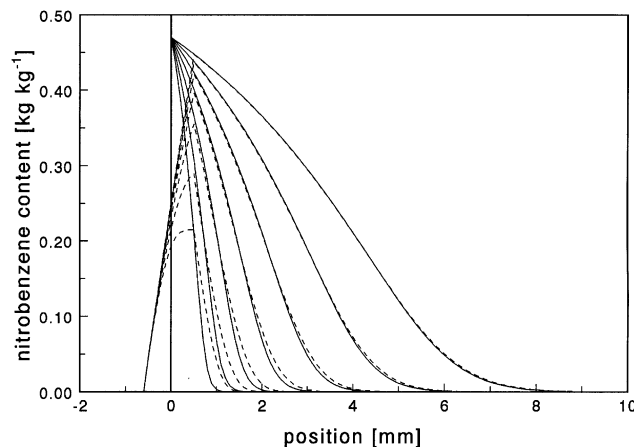


Figure 6. Simulation of the effect of the one-dimensional resolution.

The solid curves are a simulation of the ideal case with no spatial averaging; the dashed curves indicate the corresponding profiles as would have been measured using a 1-D resolution of 1 mm. The profiles are given after 1, 2, 4, 8, 16, 32 and 64 h.

at low nitrobenzene contents, it should be noted that the exact behavior of the diffusivity at these low contents has a minor effect on the adsorption process. A numerical simulation of the nitrobenzene profiles based on the diffusivity given by Eq. 11 is plotted in Figure 4. As can be seen, this simulation gives an adequate description of the measured profiles.

Error Analysis

In the determination of the effective diffusivity from the measured nitrobenzene profiles, two main causes of error can be identified, that is, the one-dimensional resolution and the noise in the nitrobenzene content measurement. Computer simulations were done to investigate the effects of these errors and to check the method that was used to calculate the effective diffusivity from the nitrobenzene profiles. First, the adsorption was simulated for an ideal sample using the effective diffusivity given by Eq. 11 with the appropriate values of D_0 and α . The simulated profiles are given by the solid curves in Figure 6. Next, the effect of the limited 1-D resolution was included by spatially averaging these results over 1 mm. The resulting profiles are indicated by the dashed curves. Indeed, the profiles show the same tendency as the experimental data plotted in Figure 3, that is, an increase in the apparent nitrobenzene content near the surface with time. The simulations reveal that for $x < 1$ mm, the nitrobenzene profiles collected up to some time after the start of the adsorption experiment are affected significantly by the limited resolution. Therefore, the data for $x < 1$ mm and the profiles collected during the first 16 h were not used for the Boltzmann transformation. Using the simulated profiles, the diffusivity was recalculated using the method discussed in the previous section. It was found that the used numerical method is only valid for nitrobenzene contents larger than $0.025 \text{ kg} \cdot \text{kg}^{-1}$. The recalculated effective diffusivity is found to reproduce the original behavior within 1%.

The results for the diffusivity using a simulation, including a 1-D resolution of 1 mm, are plotted in Figure 7. As can be

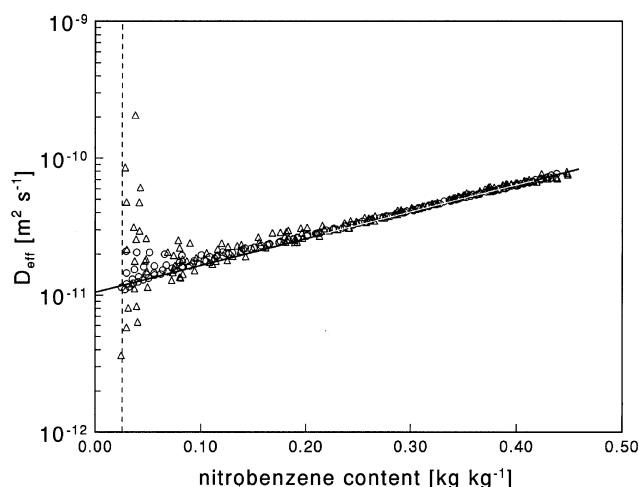


Figure 7. Effective diffusivity for adsorption as determined from the simulated profiles using an exponential approximation: $D_{\text{eff}} = 1.05 \times 10^{-11} \exp(4.5 \theta)$ (solid line).

(O) Recalculated diffusivity for a 1-D resolution of 1 mm;
(Δ) with 5% random noise added to simulated profiles.

seen, the diffusivity reproduces well, only at low nitrobenzene contents it is overestimated. To check the influence of noise, 5% random noise was added to the simulated nitrobenzene profiles. The resulting diffusivity is also plotted in Figure 7. The behavior of the original diffusivity is still well reproduced. Fluctuations occur only at lower nitrobenzene contents, which, as can be seen from a comparison of Figures 7 and 5, nicely reproduce the characteristics of the experimental results. From these simulations it can be concluded that the 1-D resolution and the presence of noise in our NMR experiments had only a minor influence on the determination of the nitrobenzene diffusivity.

Finally, simulations were also performed in order to check the influence of the mass-transfer coefficient. From these simulations it is found that the mass-transfer coefficient must be at least on the order of $10^{-6} \text{ kg} \cdot \text{m}^{-1} \cdot \text{s}^{-1}$ to justify the use of Eq. 6.

Conclusions

The adsorption process of nitrobenzene in activated carbon was studied. It has been shown that a specially adapted NMR setup can be used for determining the nitrobenzene profiles in this material during adsorption. Especially at the beginning, the measured profiles are disturbed by the limited 1-D resolution. The observed nitrobenzene transport can be modeled by a nonlinear diffusion equation. The effective diffusivity for activated carbon at 33°C can be approximated by an exponential function of the nitrobenzene content.

Acknowledgments

Part of this project was supported by the Dutch Technology Foundation (STW).

Notation

B_o = magnetic field strength, T
 D_{eff} = effective diffusivity, $\text{m}^2 \cdot \text{s}^{-1}$
 D_o = constant, $\text{m}^2 \cdot \text{s}^{-1}$
 f = resonance frequency, MHz
 l = length of the sample, m
 P = vapor pressure, $\text{N} \cdot \text{m}^{-2}$
 S = signal
 t = time, s
 T_1 = spin-lattice relaxation time, s
 T_2 = spin-spin relaxation time, s
 TE = spin-echo time, s
 TR = repetition time, s
 x = spatial coordinate, m

Greek letters

α = constant
 β = mass-transfer coefficient, $\text{kg} \cdot \text{m}^{-1} \cdot \text{s}^{-1}$
 θ = nitrobenzene content, $\text{kg} \cdot \text{kg}^{-1}$
 γ = gyromagnetic ratio, $\text{MHz} \cdot \text{T}^{-1}$
 ρ = proton density, m^{-3}

Literature Cited

- Abraham, A., *The Principles of Nuclear Magnetism*, Clarendon, Oxford (1962).
 Bear, J., and Y. Bachmat, *Introduction to Modelling of Transport Phenomena in Porous Media*, Vol. 4, Kluwer, Dordrecht, The Netherlands (1990).
 Crittenden, B., and W. J. Thomas, *Adsorption Technology and Design*, Butterworth-Heinemann, Oxford (1998).
 Kopinga, K., and L. Pel, "One Dimensional Scanning of Moisture in Porous Materials with NMR," *Rev. Sci. Instrum.*, **65**, 3673 (1994).
 Koptug, I. V., S. I. Kabanikhin, K. T. Iskakov, V. B. Fenelonov, L. Yu. Khitrina, R. Z. Sagdeev, and V. N. Parmon, "A Quantitative NMR Imaging Study of Mass Transport in Porous Solids During Drying," *Chem. Eng. Sci.*, **55**, 1559 (2000a).
 Koptug, I. V., R. Z. Sagdeev, L. Yu. Khitrina, and V. N. Parmon, "A Nuclear Magnetic Resonance Microscopy Study of Mass Transport in Porous Materials," *Appl. Magn. Resonance*, **18**, 13 (2000b).
 Pel, L., *Moisture Transport in Porous Building Materials*, PhD Thesis, Eindhoven Univ. of Technology, Eindhoven, The Netherlands (1995).
 Prado, P. J., B. J. Balcom, and M. Jama, "Single Point Magnetic Resonance Imaging Study of Water Adsorption in Pellets of Zeolite 4A," *J. Magn. Resonance*, **137**, 59 (1999).
 Schemmert, U., J. Kärger, and J. Weitkamp, "Interference Microscopy as a Technique for Directly Measuring Intracrystalline Transport Diffusion in Zeolites," *Microporous Mesoporous Mater.*, **32**, 101 (1999a).
 Schemmert, U., J. Kärger, C. Krause, R. A. Rákoczy, and J. Weitkamp, "Monitoring the Evolution of Intracrystalline Concentration," *Europhys. Lett.*, **46**, 204 (1999b).
 Wankat, P. C., *Rate-Controlled Separations*, Elsevier, New York (1990).
 Whitaker, S., "Simultaneous Heat, Mass and Momentum Transfer in Porous Media. A Theory of Drying Porous Media," *Adv. Heat Transfer*, **13**, 119 (1977).

Manuscript received Nov. 14, 2001, and revision received July 25, 2002.